Supplementary Materials and Methods

Mice. C57BL/6J mice were purchased from Jackson Laboratories (Bar Harbor, ME). Generation of mice carrying a 710 bp deletion of critical sequences in the promoter plus most of exon 1 of *H19* (H19ΔEx1) has been previously described[1]. To generate *H19* lncRNA- deficient mice and wild-type littermates, females heterozygous for the deletion ($H19^{\Delta Ex1/+}$) were crossed to male C57BL/6J mice. Since *H19* is an imprinted gene, maternal inheritance of the mutation reduces *H19* lncRNA levels by 100-fold[1]. Genotyping was carried out by PCR using a previously described protocol[1]. Co-housed age- and gender-matched wild-type littermates were used as controls. Males and females between 8 and 10 weeks of age were used for all experiments. All mice used in this study were housed in a pathogen-free animal facility and handled according to the guidelines of the National Institutes of Health. Animal husbandry was provided by trained technicians and veterinarians. All procedures involving mice were approved by the Institutional Animal Care and Use Committee of Northwestern University and conducted in compliance with the Guide for the Care and Use of Laboratory Animals 8th edition.

Human specimens. In this study, a total of 33 human colonic biopsy specimens were used. These include 16 samples from patients with ulcerative colitis (UC) and 17 samples from healthy subjects. All samples were collected with informed consent from participants. Under diagnostic colonoscopy procedures, colonic biopsies were taken from sites showing active mucosal inflammation in the sigmoid colon in subjects with UC or comparable and non-inflamed sites of colonic mucosa in subjects who were not diagnosed with the inflammatory injury in the colon. UC patients had diagnoses confirmed by physicians based on standard criteria including clinical presentation, endoscopic finding, and pathologic diagnosis. Ethical and research governance approval was provided by the Human Research Ethics Committee in Peking Union

Medical College Hospital (Beijing, China). The biopsy specimens were immersed in the RNALater solution (Ambion) and then used for RNA extraction and assessment of gene expressions by qRT-PCR.

LPS and TNF-α treatment *in vivo*. To induce an acute systemic inflammatory response, adult mice were injected intraperitoneally (i.p.) with lipopolysaccharide (LPS, 2 or 5 mg/kg; serotype 0111:B4; Sigma-Aldrich, St Louis, MO) or recombinant mouse TNF-α (2 μg per mouse; Sigma-Aldrich). Control mice were given normal saline.

Colitis and colonic mucosal wound-healing model. Adult mice were fed dextran sulfate sodium (DSS) dissolved in sterile distilled water *ad libitum* for up to 7 days followed by regular drinking water until the end of the experiment using our previously established protocol[2]. In preliminary experiments, we found DSS purchased from Gojira Fine Chemicals (Bedford Heights, OH) was more potent than DSS manufactured by MP Biomedicals (Solon, OH). Dosage regimens for the DSS treatment were 3.5% (w/v) DSS (molecular mass 36–50 kDa; MP Biomedicals) for male wild-type C57BL/6J mice, 2.0% (w/v) DSS (molecular mass 40,000; Gojira Fine Chemicals) for male $H19^{\Delta Ex1/+}$ mice and their male wild-type littermates, or 3% (w/v) DSS (molecular mass 40,000; Gojira Fine Chemicals) for female $H19^{\Delta Ex1/+}$ mice and their female wild-type littermates. The DSS solutions were made fresh on days 3 and 5. Body weight and survival were recorded daily during experiments. Animals were euthanized with CO_2 inhalation followed by cervical dislocation at the end of experiments. Colon length was measured and colon tissues were fixed in PBS-buffered 10% formalin for histopathology or processed for molecular biology studies.

Cecal ligation and puncture (CLP). Adult mice were anesthetized by i.p. injection of ketamine (100 mg/kg) and xylazine (10 mg/kg). After laparotomy, the distal portion of the

cecum (1 cm) was ligated with 5-0 silk suture. The ligated cecum was then punctured with a 21-gauge needle and slightly compressed with an applicator until a small amount of stool appeared. In sham-operated animals, the cecum was manipulated without ligation and puncture. The cecum was placed back in the peritoneum. The incision was closed using a 2-layer procedure: 7-0 fast absorbing surgical gut suture on the muscle layer and 5-0 Ethicon Mersilk Suture on the skin, respectively. Mice received an i.p. injection of saline (1 mL/mouse) for fluid resuscitation at the time of closure and Buprenex (0.05-0.10 mg/kg, in 12-hour intervals for 2 days) to minimize distress.

Histologic and microscopic analysis of colitis. The entire colon and rectum were collected, flushed with cold saline to remove any fecal content, rolled up from the proximal to the distal end in concentric circles, and fixed in PBS-buffered 10% formalin overnight. Then, tissues underwent the routine histological processing and were embedded in paraffin, sectioned, and stained with hematoxylin and eosin (H&E) in a local histology core facility. To determine the severity of colitis, H&E stained slides were evaluated by a pathologist in a blinded fashion using a histological scoring system modified from previously described criteria[3]. Briefly, the scoring system was composed of three independent parameters: severity of inflammation (0 to 3: none, slight inflammatory cell infiltration, moderate inflammatory cell infiltration, and severe inflammatory cell infiltration); depth of injury (0 to 3: none, injury restricted to the mucosal layer, injury in mucosal and submucosal layers and transmural injury); and crypt-epithelial damage (0 to 4: none, basal one-third damaged, basal two-thirds damaged, only surface epithelium intact, entire crypt and epithelium lost). The score of each parameter was multiplied by the percentage of tissue involvement. The final scores of each parameter were added to a sum that was defined as the histology score. The maximum possible histology score was 10. Images were acquired

using QCapture Suite Plus software (QImaging Corp.) with a digital camera (QImaging Retiga 4000R) and further processed by Adobe Photoshop CS6 software.

Intestinal permeability assay. At day 1 or 2 after LPS or saline treatment, mice were gavaged orally with FITC-dextran (FD4, MW 3,000-5,000, 400 mg/kg, Sigma-Aldrich). Food was withdrawn from mice 4 hours prior to gavage. At 3.5 hours after FD4 administration, mice were euthanized with CO_2 inhalation followed by cervical dislocation. Blood was collected by cardiac puncture into heparinized tubes and centrifuged at 2,000g for 10 minutes. Plasma was recovered from the supernatant and processed for measuring fluorescence intensity on a SpectraMax M5 plate reader (Molecular Devices) at 492 nm excitation/525 nm emission. A standard curve was prepared by making serial dilutions of an FD4 standard within the linear range of the curve. The concentration of FITC-dextran in plasma was calculated using the standard curve as a reference.

Cell culture. Human colonic epithelial cell line HT-29 was obtained from American Type Culture Collection (Manassas, VA). Cells were cultured in Dulbecco's Modified Eagle's Minimum Essential Medium supplemented with 10% (v/v) fetal bovine serum (FBS), 50 U/mL penicillin, and 50 μg/mL streptomycin at 37^{o}C in a humidified incubator with 5% CO_2 using our standard protocol[4].

Organoid culture, treatment, and measurement. Small intestines were isolated from wild-type or *H19*$^{\Delta Ex1/+}$ mice (male, 8 weeks), dissected and washed with DPBS 20 times. Then, the intestinal fragments were incubated with gentle a cell dissociation reagent (Stemcell Technologies, Vancouver, Canada) to separate the crypts and villi from intestinal bases. After centrifugation, the crypts were isolated and resuspended in a 1:1 mixture of Matrigel (Corning, Corning, NY) and IntestiCult^{TM} organoid growth medium (OGM, Stemcell Technologies) at a

density of 6000 crypts/mL. A droplet of 50 μL was placed into the center of a pre-warmed 24-well plate with a dome containing 300 crypts per well. After the domes were solidified, 750 μL of OGM was added to each well. Crypts were cultured at 37°C, 5% CO_2 with the medium refreshed every 3 days. To examine the expression of *H19* in response to IL22, intestinal epithelial organoids were cultured in OGM as described above for 7 days, washed with DMEM/F12, and cultured with DMEM/F12 overnight prior to IL22 treatment for an additional 6 hours followed by harvesting for RNA extraction and qRT-PCR analysis of *H19* expression. To investigate the effects of IL22 on intestine epithelial organoid growth, mouse recombinant IL22 (10 ng/mL, PeproTech, Rocky Hill, NJ) was added into the OGM. Growth of organoids was monitored continuously for 3 days under the microscope. For organoid size measurement, 15-20 random images were acquired from each treatment group with a digital camera (QImaging Retiga 4000R) and the horizontal cross-sectional surface area of the organoids was measured by Adobe Photoshop CS6 software.

Cell treatment. For *in vitro* drug treatment, $5x10^5$ HT-29 cells were seeded onto 6-well plates and cultured for 24 h with complete medium. Then, the cells were serum starved overnight prior to drug treatments in a serum-free medium. Recombinant IL22 (up to 100 ng/mL), IL-6 (50 ng/mL), IL-8 (100 ng/mL), IL-10 (10 ng/mL), IL-36α (10 ng/mL), TNF-α (100 ng/mL), IFN-γ (100 ng/mL), TGF-β1 (5 ng/mL), EGF (100 ng/mL), FGF-2 (10 ng/mL), Leptin (100 ng/mL) and Oncostatin-M (OSM, 100 ng/mL) were purchased from PeproTech. Chemicals including S1P (3 μmol/L), PGE2 (1 μmol/L), 8-Bromo-cAMP (1 mmol/L), epinephrine (100 ng/mL), norepinephrine (100 ng/mL), S3I-201 (100 μmol/L), H89 (up to 10 μmol/L), Rp-CAMPS (10 μmol/L), and forskolin (20 μmol/L) were obtained from Cayman Chemical. Isoproterenol (100 μmol/L) was purchased from EMD Millipore and dideoxyforskolin (DDFK,

20 μmol/L) was obtained from Sigma-Aldrich. PKI (14-22, 10 μmol/mL), a peptide inhibitor bound to the catalytic subunit PKA[5], was purchased from Santa Cruz Biotechnology. The concentrations stated in parentheses specify the doses of drugs used in cell culture experiments.

Generation of HT-29 cells with stable overexpression of human *H19*. The overexpression of *H19* in HT-29 cells was achieved using a lentiviral vector-mediated gene transfer technology. Briefly, the full-length human *H19* cDNA (GE Healthcare Bio-Science) were subcloned into a pLVX-Puro vector (Clontech). A list of the primers used is provided in **Supplementary Table 3**. Lentivirus particles were generated by transfection of HEK293T cells (ATCC) with a plasmid mixture containing pLVX-Puro plasmid bearing the human *H19* cDNA and packaging plasmids including psPAX2 and pMD2·G (Addgene) using Lipofectamine 3000 (Life Technologies) according to the manufacturer's instructions. The supernatant was collected after a 48-hour transfection and used as viral stocks. HT-29 cells were transduced with lentivirus particles containing the pLVX-Puro vector bearing human *H19* cDNA followed by treatment with puromycin (2 μg/ml) for 2 weeks. The overexpression of human *H19* in the transduced cells was confirmed by the qRT-PCR assay. Cells with stable overexpression of human *H19* were named HT-29^{H19OE}. Control cells were transduced with lentivirus particles containing empty pLVX-Puro vector and named HT-29^{EV}.

Protein kinase A (PKA) activity assay. HT-29 cells were lysed with RIPA lysis buffer containing protease inhibitor cocktails (Sigma-Aldrich) and Halt phosphatase inhibitor cocktail (Thermo-Fisher). Cell lysates were centrifuged at 10,000g for 10 minutes at 4^{o}C. The supernatants were processed for measurement of PKA kinase activity in triplicate using a non-radioactive PKA assay kit (Enzo Life Sciences) according to the manufacturer's instructions.

***Ex vivo* mouse intestinal explant culture**. The method was modified from a previously described protocol[6]. Briefly, fresh small intestines were flushed with cold PBS, opened along the longitudinal axis, washed with sterile Dulbecco's Modified Eagle Medium/Nutrient Mixture F-12 (DMEM/F12, without phenol red) 3 times, and cut into 4-mm square pieces. The small intestine tissue pieces were laid on 24-mm Netwell™ inserts with 500 μm polyester mesh bottoms (Corning) with the serosal layer facing to the bottom of the inserts. The inserts were placed into 6-well microplates. Phenol red-free DMEM/F12 culture medium containing penicillin (100 IU/mL, Corning), streptomycin (100 μg/mL, Corning) and Polymyxin B (100 IU/mL, Sigma-Aldrich) was slowly added to the microplates until the liquid layer just reached the mucosal surface of the tissue pieces. The Netwell™ insert-microplate sets containing intestine explants were pre-incubated at 37^{o}C in a humidified incubator with 5% CO_2 for 1 hour. Then, IL22 (100 ng/mL) was added to the culture medium and intestinal explants were cultured at 37^{o}C in a humidified incubator with 5% CO_2 for 4 hours followed by RNA extraction and qRT-PCR to measure gene expressions.

Total RNA extraction and real-time quantitative RT-PCR (qRT-PCR). Total RNA was extracted from tissue or cells using Trizol reagent (Life Technologies), RNA was quantified with the Nanodrop instrument (Agilent Technologies), single strand cDNA was generated using the iScript cDNA synthesis kit (Bio-Rad), and relatively quantitative real-time PCR was performed using SYBR Green PCR Universal Mastermix (Life Technologies) and Fast 7500 real-time PCR system (Applied Biosystems), all according to the manufacturers' manuals. Fold changes in expression levels of *H19* were calculated by $2^{-\Delta\Delta CT}$ method using GAPDH as an endogenous reference. The PCR reaction was run in duplicate for each sample. Primers used in qRT-PCR were synthesized by Integrated DNA Technologies, Inc (IDT). A list of the primers

used in these studies is provided in **Supplementary Table 3**. In some experiments, miRNA expression was examined using the TaqMan microRNA assay system (Life Technologies). Briefly, for each specific miRNA examined, target-specific stem-loop reverse transcription was employed using total RNA as the template by TaqMan microRNA reverse transcription kit (Life Technologies), and quantitative PCR was performed using the TaqMan microRNA assay together with the TaqMan universal PCR master mix (Life Technologies), all according to the manufacturers' protocols. Fold changes in miRNA expression levels were determined by $2^{-\Delta\Delta CT}$ using RNU48 (for human) or snoRNA202 (for mouse) as an endogenous reference, respectively.

RNA sequencing (RNA-Seq). Mice were treated with either saline or LPS (2 mg/kg, i.p.) for 24 hours (3 mice per group). Total RNA was extracted from the small intestine using Trizol reagent followed by DNase treatment and purification, RNA integrity and quantity were assessed using an Agilent 2100 Bioanalyzer (Agilent Technologies), and total RNA (5 μg) was processed for removal of rRNA using Ribo-Zero Gold Kit (Illumina). Following rRNA removal, the RNA samples were used to prepare cDNA libraries using NEBNext Ultra RNA Library Prep Kit (Illumina), all steps were completed according to the manufacturers' manuals. The cDNA libraries were pair-end sequenced (2x100 bp) on Illumina HiSeq 2000 platforms in a local genomics core facility. The RNA-seq data were processed to generate pre-processed FATSQ files exhibiting the same indexes, followed by a merge-process using CASAVA Pipeline (Illumina). The FASTQ sequences were then aligned to a reference mouse genome annotation (GENCODE version M11). The alignment was performed using HISAT2 software (version 2.0.5) with default parameters. The aligned sequences were further sorted with Samtools (version 1.3.1). The expression quantification counting was performed using HTSeq-count (version 0.6.1) using a reference mouse genome annotation (GENCODE version M11) with

parameter '–s no' in default union mode. The count matrix was then normalized and differentially expressed genes were identified with the DESeq2 package (version 1.14.1) in R/Bioconductor software (version 3.3.2). The GO analysis was performed with GOTERMFINDER developed at the Lewis-Sigler Institute at Princeton[7]. A total of714 differentially expressed protein coding and non-coding genes (cut-off *P*-value = 0.05) were identified from the RNA-Seq results (Control vs. LPS) as the input list. Significant GO terms shared among these genes were summarized using GOTERMFINDER, with default Bonferroni correction for p-values ($P < 0.01$).

***In situ* hybridization (ISH)**. A 506 bp sequence of mouse *H19* cDNA was generated with RT-PCR from intestinal total RNA of LPS-treated mice using the m*H19*-ISH-F1, m*H19*-ISH-R1 primer set (**Supplementary Table 3**). The cDNA fragment was TA cloned into the pGEM-T vector (Promega) and forward insertion was verified by DNA sequencing. The new construct, pGEM-m*H19*, was utilized as a template for PCR to generate a mouse *H19* cDNA fragment containing the SP6 promoter at the 5'-end of the antisense strand using the m*H19*-ISH-F1, M13 reverse primer set (**Supplementary Table 3**). The PCR product was processed to generate DIG-labeled antisense RNA probes against mouse *H19* using a DIG RNA labeling kit by SP6 RNA polymerase (Roche Diagnostics) according to the manufacturer's manual. The *in situ* hybridization procedure was a modification of a previously described method[8]. Briefly, fresh mouse tissues were fixed in 4% paraformaldehyde overnight and processed for paraffin embedding in a local histology core facility. Paraffin-embedded tissues were sectioned at 5 μm thickness onto plus (+) slides, deparaffinized in xylene and rehydrated in graded ethanol and RNase-free deionized Millipore water. Prior to hybridization, sections were digested with proteinase K (20 mg/mL) for 20 minutes at 37^{o}C and acetylated in 0.25% acetic anhydride in 0.1

mol/L triethanolamine (pH 8.0). Sections were prehybridized in 50% (v/v) deionized formamide in 2X SSC at 58°C for 2 hours and then hybridized overnight at 55°C in a humidified chamber with hybridization buffer containing DIG-labeled antisense *H19* probe (2 ng/μL), 50% (v/v) deionized formamide, 1X Denhardt's solution, yeast tRNA (0.3 mg/mL), 5X SSC, 5% dextran sulfate, 0.1% CHAPS, 0.1% Tween 20, and EDTA (5 mmol/L, pH 8.0). After hybridization, sections were briefly washed with 2X SSC followed by treatment with RNase A (10 μg/mL) for 1 hour at 37°C. Then, slides were washed sequentially with 2X SSC at 55 – 60°C for 20 minutes, 0.2X SSC at 55 – 60°C for 20 minutes, and PBS briefly at room temperature. To detect DIG-labeled antisense RNA probes, slides were incubated with the alkaline phosphatase-conjugated anti-DIG antibody (Cat# NEF832001, Perkin Elmer), treated with a TSA amplification kit (Perkin Elmer), and developed with NBT/BCIP (Roche Diagnostics), all according to the manufacturers' manuals. Finally, slides were counterstained with Nuclear Fast Red (Sigma-Aldrich) and mounted for examination under a microscope. Images were acquired using QCapture Suite Plus software (QImaging Corp.) with a digital camera (QImaging Retiga 4000R) and further processed by Adobe Photoshop CS6 software.

Dual-fluorescent *in situ* hybridization (RNAscope assay). The cellular localization of Lgr5 mRNA and *H19* transcripts in mouse intestine tissues were determined using RNAscope Multiplex Fluorescent Reagent Kit v2 (Advanced Cell Diagnostics, Hayward, CA). The manufacture's instruction was followed. Briefly, mouse small intestinal tissues were fixed in 10% neutral buffered formalin overnight, processed for standard paraffin embedding, and sectioned in 5-μm thickness. The tissue sections were deparaffinized in xylene and rehydrated in graded ethanol and RNase-free deionized Millipore water. Prior to hybridization, tissue sections were pretreated with boiled target retrieval buffer supplied in the kit for 15 minutes followed by

protease plus treatment for 30 minutes at 40°C. Sections were then hybridized for 2 hours at 40°C in a hybridization oven (Labnet International Inc., Edison, NJ) with a mixture containing the hybridization buffer supplied in the kit and RNAscope probes for mouse Lgr5 mRNA and *H19* transcripts (Cat No. 312171 and 423751-C2, Advanced Cell Diagnostics) followed by successive incubations with amplifier reagents Amp1 to 3 accordingly. After treatment with amplifier reagents, probe-Lgr5 hybrids and probe-*H19* hybrids were visualized using TSA Plus Fluorescein system (Cat No. NEL741E001KT, PerkinElmer) and TSA Plus Cyanine 3 system (Cat No. NEL744E001KT, PerkinElmer) respectively. Finally, slides were mounted with the antifade mounting media containing 4', 6-diamidino-2-phenylindole (DAPI, Vector Lab, Inc. Burlingame, CA). The microscopy images of 12 series coronal sections per intestinal crypt area were acquired as z-stacks with 0.33 μm z-spacing on a ZEISS LSM 880 Confocal Laser Scanning Microscope equipped with AiryScan and a PlanApo 63x/1.4 oil immersion objective (Carl Zeiss Microscopy GmbH, Jena, Germany). Fluorescein (Lgr5), Cy3 (*H19*), and DAPI (nuclei) were excited at 488, 561, 405 nm respectively. Images were processed using Zeiss ZEN 2 Core Microscopy Software. To analyze z-stacks as one image composed of all superimposed confocal slices rather than several images individually, we used Adobe Photoshop CS6 software to project the z-stack images into a 2D plane.

Immunofluorescent staining. Paraffin-embedded tissue sections (5 μm) were deparaffinized in xylene and rehydrated in an alcohol series. Sections were subjected to epitope retrieval by boiling for 30 minutes in a buffer containing 10 mmol/L sodium citrate buffer (pH 6.0) and 0.05% (v/v) Tween 20 followed by slow cooling to room temperature. Sections were blocked with PBS containing 1% BSA and 2% normal goat serum (Vector Labs, Burlingame, CA) for 1 hour at room temperature and incubated at 4°C overnight with primary antibodies,

including rat anti-BrdU (1:100; Cat# OBT00306, Bio-Rad), rat anti-Ki-67 (1:200, Cat# 14-5698-82, Affymetrix), rabbit anti-Mycn (C-19, 1:50, Cat# SC-791, Santa Cruz), rabbit anti-FoxM1 (K-19, 1:100, Cat# SC-500, Santa Cruz). After incubation, slides were washed with PBS and subsequently incubated for 1 hour at room temperature in the dark with appropriate secondary antibodies, including goat anti-rabbit IgG antibody labeled with Alexa Fluor 488 (1:250; Cat# A11034, Life Technologies), goat anti-rat IgG antibody labeled with Alexa Fluor 488 (1:250; Cat# A-11006, Life Technologies), or goat anti-rat IgG antibody labeled with Alexa Fluor 594 (1:250; Cat# A-11007, Life Technologies). Finally, slides were washed with PBS and mounted with 4',6-diamidino-2-phenylindole (DAPI)-contained mounting solution (Vector Labs). Slides were reviewed under an upright fluorescence microscope (model MD R; Leica Microsystems). Images were acquired using image software Openlab with a digital camera (QImaging Retiga 4000R) and further analyzed by Adobe Photoshop CS6 software.

Measurement of proliferation and migration of crypt epithelial cells in the small intestine with a 5-bromo-2'-deoxyuridine (BrdU) pulse-chase assay. The method for labeling proliferative epithelial cells in crypts with BrdU was modified from a previously described protocol[9]. Briefly, mice were i.p. injected with BrdU (50 mg/kg; BD Biosciences) 18 hours after LPS (2 mg/kg, i.p.) treatment and euthanized with CO_2 inhalation 1 hour after BrdU was given. The entire small intestine was removed, flushed with cold saline, fixed with 10% buffered formalin, handled with a routine histological process, and embedded in paraffin. Tissue sections (5 μm) were subjected to immunofluorescent staining with anti-BrdU antibody as described above followed by examination under a fluorescent microscope in the low power field of view (X10). The number of BrdU-positive cells per crypt was counted for 5 random fields per mouse and averaged. An average of 15 crypts were counted per animal in a blinded manner. To

measure the intestinal enterocyte migration along the crypt-villus axis, mice were i.p. injected with BrdU (50 mg/kg) at 8 hours after LPS (2 mg/kg, i.p.) treatment and sacrificed with CO_2 inhalation 36 hours after BrdU was given. The intestinal tissue samples were processed and stained with anti-BrdU antibody as described above. Under a fluorescent microscope in the low power field of view (X10), images from 5 random fields per mouse were acquired using image software Openlab with a digital camera (QImaging Retiga 4000R). The distance of enterocyte migration was determined by measuring the gap between the crypt base and the highest labeled cell within the crypt-villus axis using Adobe Photoshop CS6 software. An average of 15 crypt-villus axes were examined per animal in a blinded manner and the mean migration distance was used in subsequent analyses.

Assessment of colonic epithelial cell regeneration. Adult mice were subjected to acute colitis and mucosal wound-healing model with 2% (v/v) DSS treatment for 5 days and normal drinking water for 3 days. Then, mice were i.p. injected with BrdU (50 mg/kg) 1 hour prior to sacrifice. After euthanasia, the entire colon tissue was removed, flushed with cold saline, fixed with 10% buffered formalin, handled with a routine histological process, and embedded in paraffin. Tissue sections (5 μm) were subjected to immunofluorescent staining with anti-BrdU antibody as described above followed by examination under a fluorescent microscope in the low power field of view (X10). A total of three views (distal, middle, and proximal colons) were captured under an upright fluorescent microscope. The numbers of regenerated epithelial clusters (REC) were counted. Colonic epithelial cell regeneration was expressed as a number of REC per millimeter colon length.

Immunoprecipitation of p53-*H19* complexes. The Magna RNA-binding protein immunoprecipitation (RIP) assay kit (Millipore) was used for the assay. Briefly, cells were lysed

in a buffer containing protease inhibitor cocktail and RNase inhibitor. The cell lysates (100 μL from 2 X 10^7 cells per RIP reaction) were processed for the RIP assay using rabbit anti-p53 antibody (Cat# SC-126X, Santa Cruz) according to the manufacturer's protocol. The antibody-bound protein/RNA complexes were recovered using magnetic Protein A/G beads (Millipore). Co-precipitated RNA was purified and reverse transcribed using the standard protocol described above followed by measurement of p53-bound *H19* lncRNA by qRT-PCR.

Dual-luciferase assay for measuring p53 activity. Cells were co-transfected with 100 ng p53 luciferase reporter plasmid (PG13-luc) which possesses p53 binding sites in cis (Addgene) together with 40 ng pRL-TK-Renilla-luciferase plasmid (Promega) using Lipofectamine 3000 (Life Technologies). Forty-eight hours post-transfection, cells were lysed and the cell lysates were processed for measurement of luciferase activity using a dual-luciferase reporter assay system (Promega) according to manufacturer's standard protocol.

***In-silico* analysis for determining cell growth-associated *H19*-binding miRNAs**. Mouse and human *H19* sequences were respectively scanned for perfect matches against the miRNA seed sequences using the FindTar3 Online Prediction program (http://bio.sz.tsinghua.edu.cn/content/index). From predicted *H19*-binding miRNAs, the cell growth-associated miRNAs were characterized using the OncomiRDB online database (http://bioinfo.au.tsinghua.edu.cn/member/jgu/oncomirdb/index.php).

RNA antisense purification (RAP) assay. Total RNAs extracted from the small intestines of mice treated with LPS or saline were used for the assay. The procedure was a modification of a previously described protocol[10]. Briefly, a set of two single-stranded DNA (ssDNA) oligo probes with a biotin-labeled 5'-end were synthesized by Integrated DNA Technologies, Inc. Each oligonucleotide probe contained 90 nucleotides complementary to a

region of mouse *H19* lncRNA (**Supplementary Table 3**). The sequences of oligo probes did not overlap each other. For the RAP assay, RNA samples (40 μg) suspended in 50% formamide were incubated at 65 °C for 10 min followed by rapid chilling on ice for denaturing, and a biotinylated *H19* ssDNA probe mixture (25 pmol for each probe) suspended in 50% formamide was incubated at 68 °C for 10 minutes followed by rapid chilling on ice. The denatured RNA samples and probes were combined and processed for hybridization at 50°C for 3 hours in a buffer containing 50% formamide, 5X SSC, and 5 mmol/L EDTA (pH8.0). The ssDNA probe-*H19*-miRNA complexes were captured by MyOne Streptavidin C1 Dynabeads (Life Technologies), washed, and eluted according to the manufacturer's instruction. Elutes were purified using RNA clean and concentrator column (Zymo Research) and processed for measuring *H19*-binding miRNAs including let-7e, let-7g, let-7i, and Mir34a using the TaqMan microRNA assay system (Life Technologies).

Protein isolation and Western blotting assay. Cells were lysed with RIPA lysis buffer (Thermo Fisher Scientific) containing a cocktail of protease inhibitors (Sigma-Aldrich). Lysates were spun at 10,000g for 10 minutes at 4°C. The protein concentration in the supernatants was determined using Pierce BCA protein assay kit (Thermo Fisher Scientific). For Western blotting, equal amounts of each protein sample (25 μg) were loaded and separated in 4-20% TGX precast SDS-PAGE gels (Bio-Rad) followed by transfer onto PVDF membranes (Bio-Rad). The membrane was blotted with anti-FOXM1 (1:1000, Cat# 5436S, Cell Signaling) or anti-MYCN (1:1000, Cat# Ab24193, Abcam) at 4 °C overnight, followed by incubation with secondary antibodies at room temperature for 1 hour. The immune complexes on blots were developed with an ECL kit (Thermo Fisher Scientific) and visualized by the Bio-Rad ChemiDoc MP System (Bio-Rad). For detection of house-keeping gene expression, blots were stripped and re-

probed with an HRP-conjugated antibody against β-actin (1:50,000, Cat# A3854, Sigma-Aldrich) followed by development with the ECL kit, scanning and analyzing as described above.

Statistical analysis. For *in vivo* experiments, sample sizes were estimated based on our pilot studies and no mice were excluded from experiments. *In vitro* experiments were performed at least twice with duplicate samples. Statistical analysis was performed with GraphPad Prism 6 software or SPSS. Data are presented as mean ± SEM. Groups were compared using the two-tailed Student's *t*-test for parametric data. When comparing multiple groups, data were analyzed by one-way analysis of variance (ANOVA) followed by Tukey's post-hoc test. Correlation of variables was determined by Pearson correlation coefficient. Kaplan–Meier survival analysis was performed and the a log-rank test was used to compare survival between groups. A two-sided $P < 0.05$ was considered to represent a statistically significant difference. All the variances were similar between groups that were statistically compared.

References

1. Srivastava M, Frolova E, Rottinghaus B, et al. Imprint control element-mediated secondary methylation imprints at the Igf2/H19 locus. J Biol Chem 2003;278:5977-83.
2. Chogle A, Bu HF, Wang X, et al. Milk fat globule-EGF factor 8 is a critical protein for healing of dextran sodium sulfate-induced acute colitis in mice. Mol.Med. 2011;17:502-507.
3. Krieglstein CF, Anthoni C, Cerwinka WH, et al. Role of blood- and tissue-associated inducible nitric-oxide synthase in colonic inflammation. Am.J.Pathol. 2007;170:490-496.
4. Bu HF, Wang X, Tang Y, et al. Toll-like receptor 2-mediated peptidoglycan uptake by immature intestinal epithelial cells from apical side and exosome-associated transcellular transcytosis. J.Cell.Physiol. 2010;222:658-668.
5. Knighton DR, Zheng JH, Ten Eyck LF, et al. Structure of a peptide inhibitor bound to the catalytic subunit of cyclic adenosine monophosphate-dependent protein kinase. Science 1991;253:414-20.
6. Yan F, Cao H, Cover TL, et al. Soluble proteins produced by probiotic bacteria regulate intestinal epithelial cell survival and growth. Gastroenterology 2007;132:562-75.
7. Boyle EI, Weng S, Gollub J, et al. GO::TermFinder--open source software for accessing Gene Ontology information and finding significantly enriched Gene Ontology terms associated with a list of genes. Bioinformatics 2004;20:3710-5.
8. Cox KH, DeLeon DV, Angerer LM, et al. Detection of mrnas in sea urchin embryos by in situ hybridization using asymmetric RNA probes. Dev Biol 1984;101:485-502.
9. Barker N, van Es JH, Kuipers J, et al. Identification of stem cells in small intestine and colon by marker gene Lgr5. Nature 2007;449:1003-7.

10. Engreitz J, Lander ES, Guttman M. RNA antisense purification (RAP) for mapping RNA interactions with chromatin. Methods Mol Biol 2015;1262:183-97.

SUPPLEMENTAL FIGURES

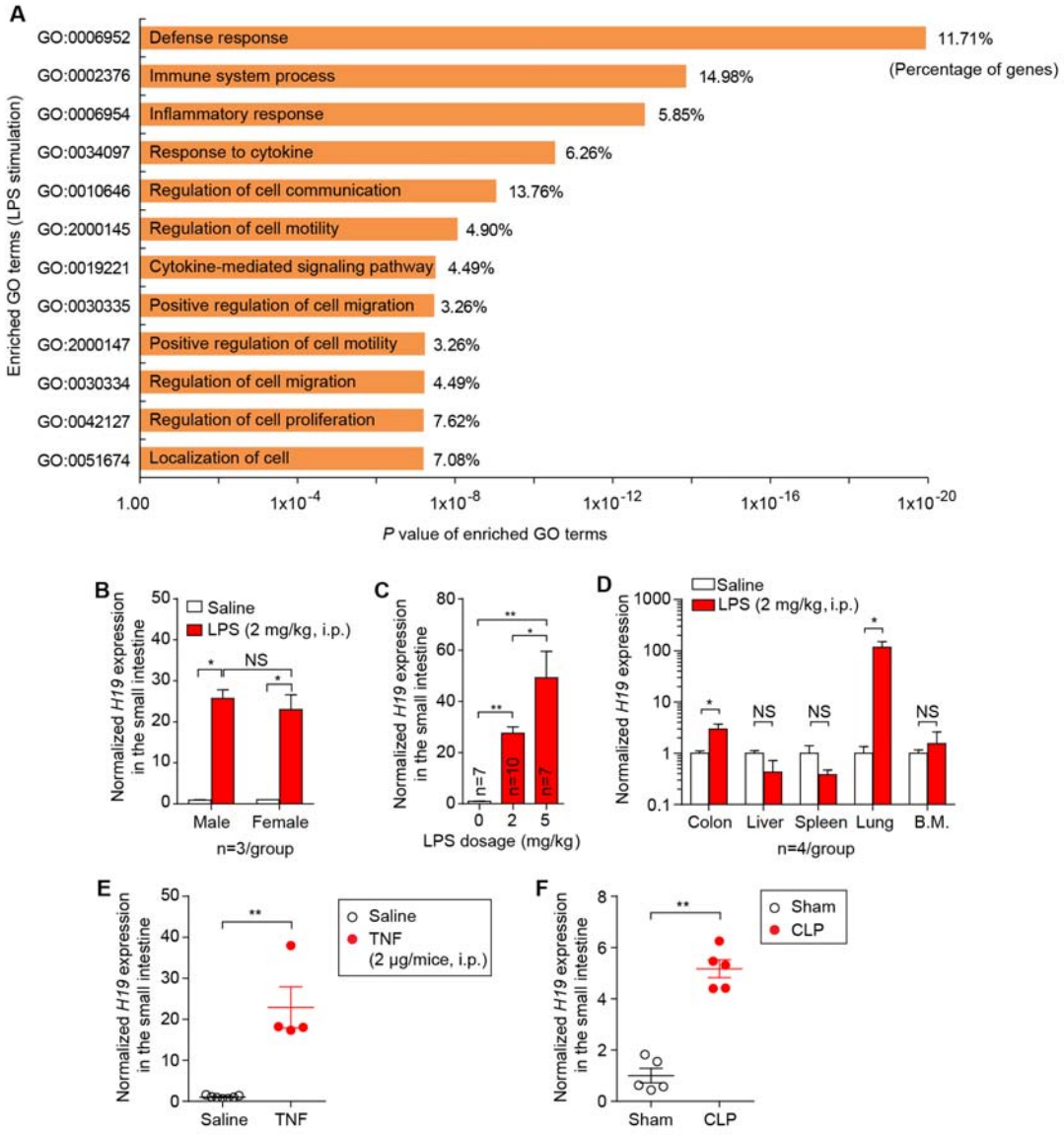

Supplementary Figure 1. Effect of systemic inflammation on *H19* expression. (***A***) GO analysis of protein-coding genes altered in the small intestine of C57BL/6J mice (male, 10 weeks old) treated with LPS (2 mg/kg, i.p.) vs. controls at 24 hours. (***B–D***) Additional results from qRT-PCR analysis reveals that LPS treatment induces intestinal *H19* expression at 6 hours in both male and female mice (***B***) in a dose-dependent (***C***) and tissue-specific (***D***) manner. B.M., bone marrow. (***E***, ***F***) Intestinal *H19* expression in mice (male, 10 wks old) at 6 h after treatment with TNF (***E***) or at 24 hours after CLP (***F***). qRT-PCR assay. CLP, cecal ligation and puncture. Bars, mean ± SEM. **P* < 0.05, ***P* < 0.01, NS = not significant.

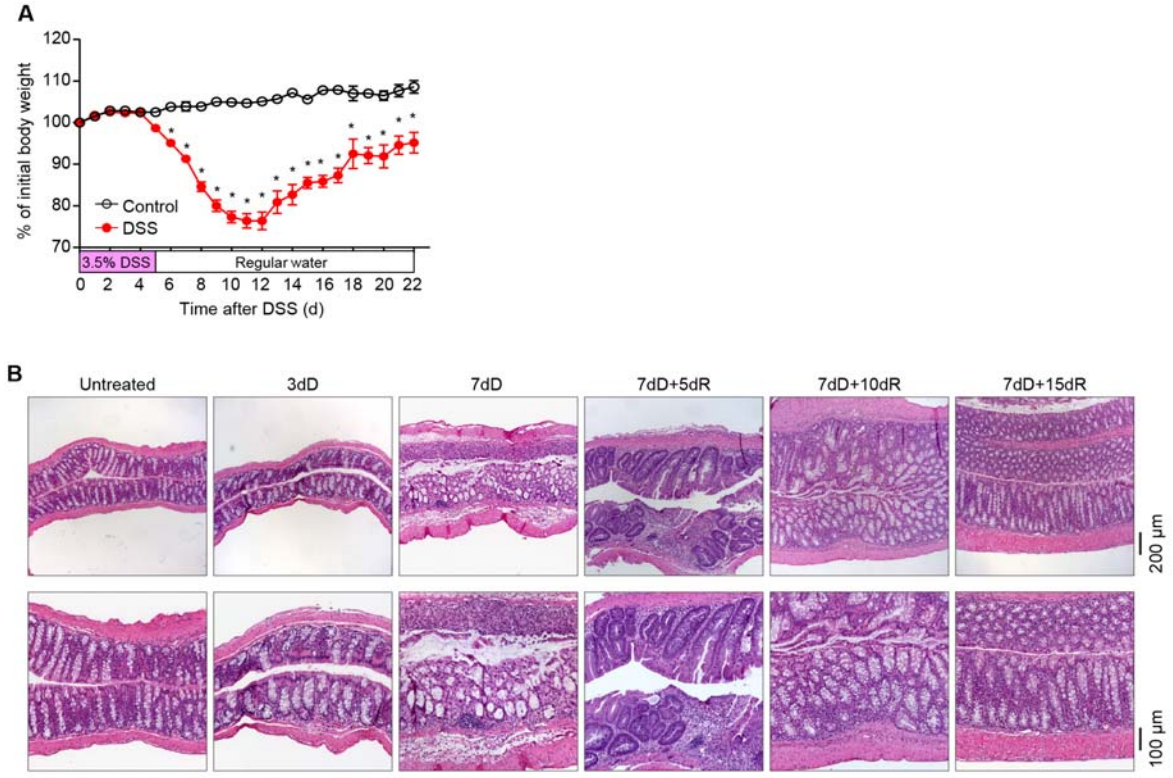

Supplementary Figure 2. Modeling of wound-healing of colonic mucosa using DSS exposure-water recovery treatment scheme. (***A***, ***B***) The change in body weight (***A***) and colonic histology (***B***) over the course of DSS (MP Biomedicals) treatment and after replacement with distilled water. Bars, mean ± SEM. **P* < 0.05, ***P* < 0.01. n = 5 mice per condition. The representative images from five micrographs of colonic histology (hematoxylin and eosin staining) are shown. dD, days of DSS treatment; dR, days of recovery.

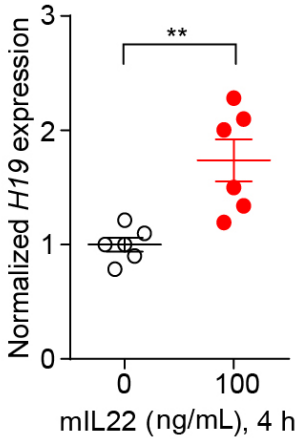

Supplementary Figure 3. Effect of IL22 on *H19* expression in mouse intestine explant culture. Mouse intestine explants were cultured with or without IL22 (100 ng/mL) for 4 hours followed by qRT-PCR analysis of *H19* expression. Bars, mean ± SEM. $^{**}P < 0.01$.

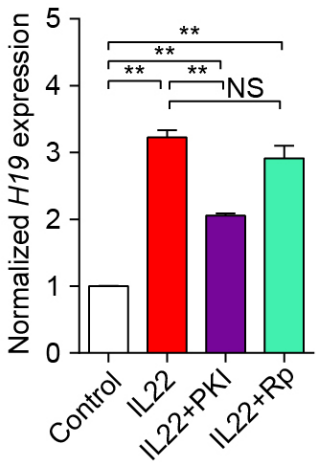

Supplementary Figure 4. Effect of PKA inhibition with PKA inhibitors targeting different subunits of PKA on IL22-induced *H19* expression in HT-29 cells. HT-29 cells were subjected to indicated treatments. The inhibitors (10 μmol/L) were added to culture medium at 30 minutes before IL22 (50 ng/mL) treatment. IL22 treatment was employed for 90 minutes. At the end of treatments, cells were processed for RNA extraction followed by measuring *H19* expression with qRT-PCR. $n = 4$ each. Bars, mean ± SEM. $^{*}P < 0.05$, $^{**}P < 0.01$, NS = not significant. PKI (14-22) is a synthetic peptide with highly specific inhibitory activity to PKA catalytic subunit), whereas Rp (i.e. Rp-cAMPS) is a PKA inhibitor blocking cAMP-binding sites.

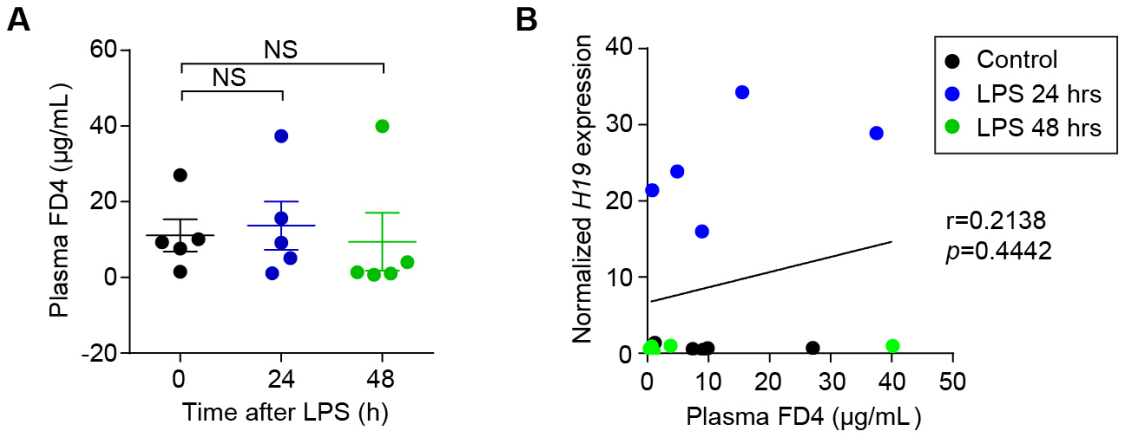

Supplementary Figure 5. LPS-induced increase in intestinal *H19* is not associated with alteration of intestinal permeability. (***A***) Mice were subjected to LPS treatment (2 mg/kg, i.p.) and sacrificed at the indicated time points, then gavaged with fluorescein isothiocyanate-dextran 4 kDa (FD4) 3.5 hours prior to sacrifice. Intestinal mucosa-to-blood permeability was assessed by measuring FD4 concentration in the plasma. (***B***) Statistical analysis shows no correlation between intestinal *H19* levels and intestinal permeability in mice after LPS treatment. Pearson correlation coefficients (r) and *P* values are indicated. NS = not significant.

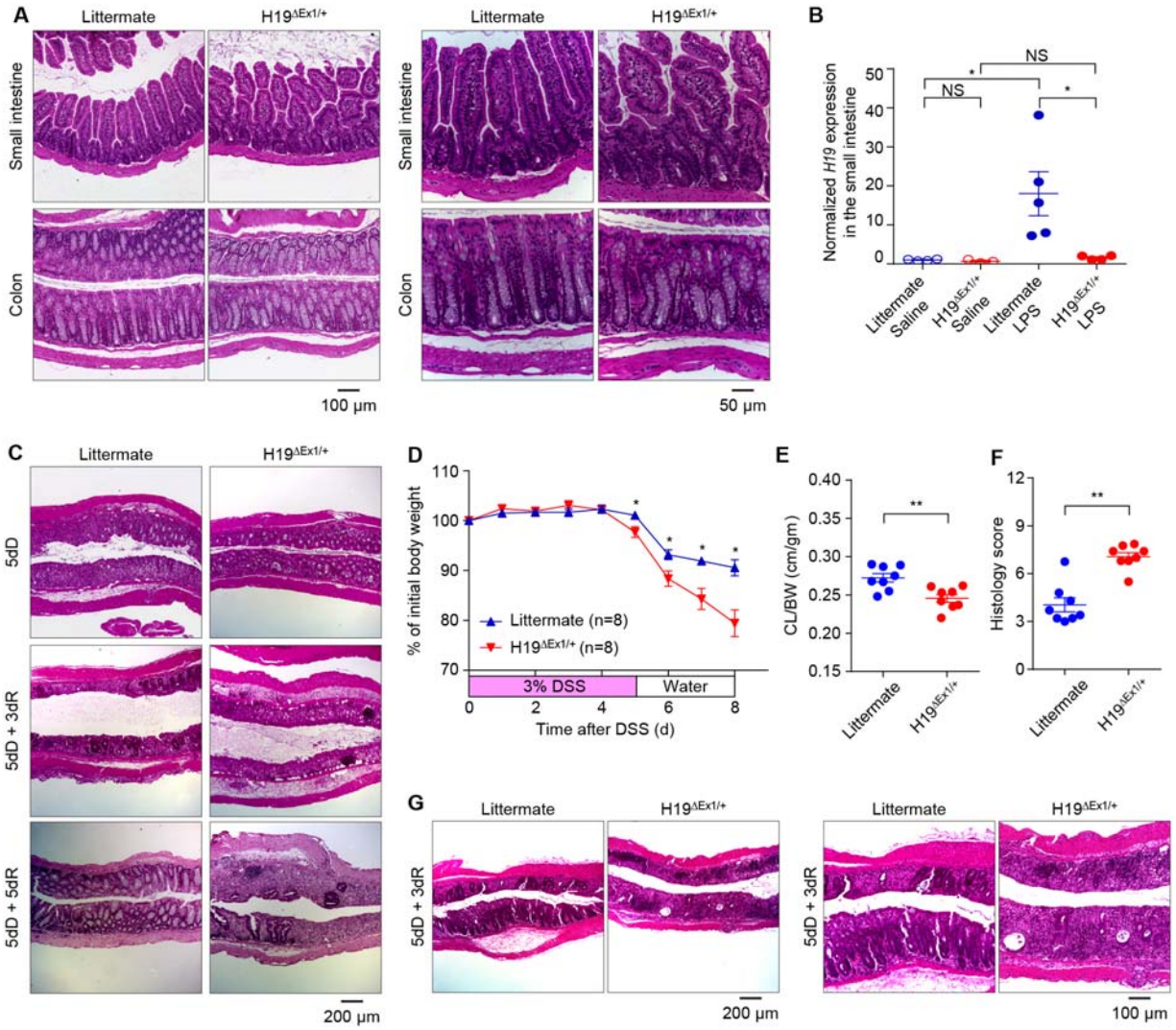

Supplemental Figure 6. ***H19*** **deficiency does not influence intestinal histology but does impair healing of the intestinal mucosa in mice with DSS-induced colitis**. (***A***) H & E-stained intestinal tissues of $H19^{\Delta Ex1/+}$ mice and their wild-type littermates (male, 10 weeks old). Representative images of five micrographs are shown. (***B***) qRT-PCR assay reveals that maternal deletion of *H19* attenuated the effect of LPS on induction of intestinal *H19* expression. Bars, mean ± SEM. **P* < 0.05. Sacrificed at 6 hours post-LPS (2 mg/kg, i.p.) or saline treatment. (***C***) Additional histological analysis of colonic mucosal histology in male $H19^{\Delta Ex1/+}$ mice and their wild-type littermates subjected to DSS-water treatment scheme. Representative images of five micrographs H&E stained colon sections in each group were shown. (***D***–***G***) Comparison of changes in body weight (***D***), colon length-to-body weight ratio (CL/BW) (***E***), histology score for mucosal injury (***F***), and colonic histology (H&E staining) (***G***) at the indicated time periods of the DSS-water treatment scheme, comparing female $H19^{\Delta Ex1/+}$ mice and their female wild-type littermates. dD, days of DSS treatment. dR, days of recovery. Bars, mean ± SEM. **P* < 0.05, ***P* < 0.01, NS = not significant. DSS (molecular mass 40,000) purchased from Gojira Fine Chemicals was used.

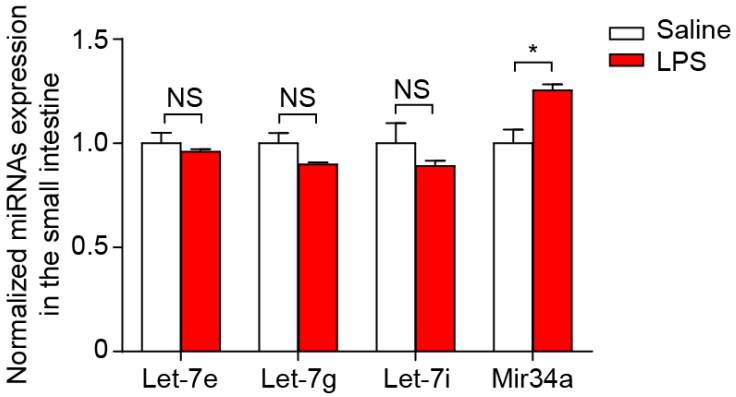

Supplementary Figure 7. Effect of LPS treatment on intestinal let-7 and Mir34a expressions. qRT-PCR analysis of miRNA expressions in the small intestine of mice 18-hours after treatment with LPS (2 mg/kg, i.p.) or saline. Bars, mean ± SEM. **P* < 0.05, NS = not significant.

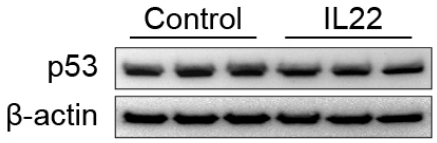

Supplementary Figure 8. Effect of IL22 treatment on p53 protein expression in HT-29 cells. HT-29 cells were treated with IL22 (50 ng/mL) for 24 hours. The control cells were treated with culture medium alone. At the end of treatments, cells were processed for isolation of total protein followed by measuring p53 protein expression with Western blot.

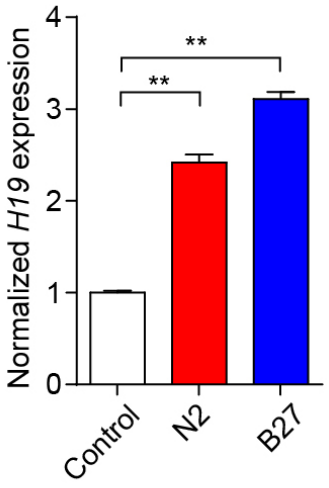

Supplementary Figure 9. Effect of cell growth supplements on *H19* expression in intestinal epithelial cells. HT-29 cells were cultured with the indicated medium for 6 hours followed by qRT-PCR analysis of *H19* expression. Bars, mean ± SEM. $^{**}P < 0.01$.

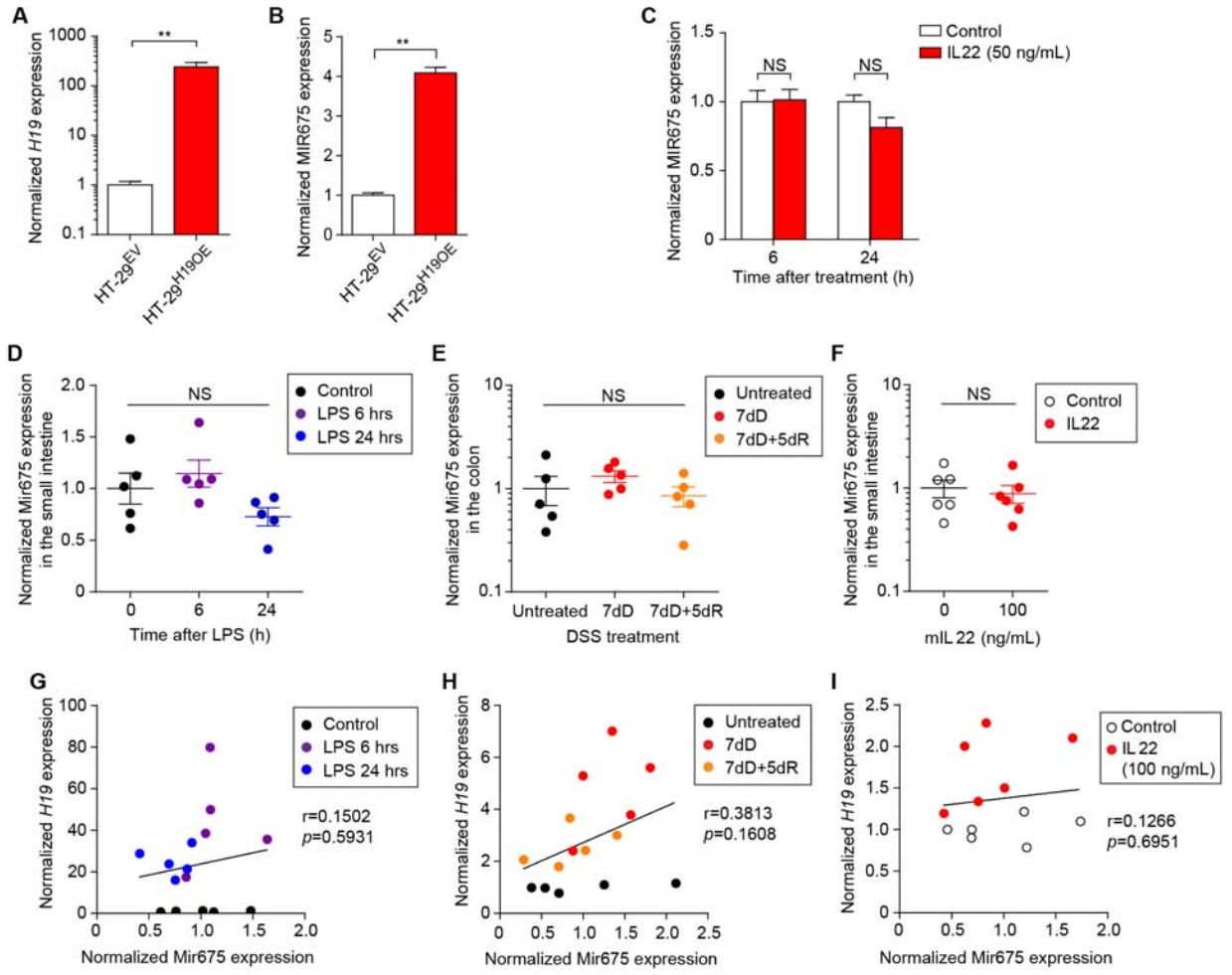

Supplementary Figure 10. Lack of the correlation between intestinal *H19* expression and microRNA 675 levels under inflammatory conditions. (***A***) qRT-PCR assay reveals an increase of *H19* expression in HT-29^{H19OE} cells (HT-29 cells transduced by lentivirus containing pLVX-Puro vector bearing human *H19* cDNA) vs. HT-29^{EV} cells (HT-29 cells transduced by lentivirus containing pLVX-Puro vector). (***B–F***) qRT-PCR assay of microRNA 675 expression in HT-29^{H19OE} and HT-29^{EV} cells (***B***), HT-29 cells with indicated treatments (***C***), the small intestines of LPS-treated mice (***D***), the colons of DSS-treated mice (***E***), and IL22-treated intestine explant culture (***F***). (***G–I***) Assessment of the correlation between *H19* and Mir675 levels in the small intestines of LPS-treated mice (***G***), the colons of DSS-treated mice (***H***), and IL22-treated intestine explant culture (***I***). Pearson correlation coefficients (r) and *P* values are indicated. Bars, mean ± SEM. $^{**}P < 0.01$, NS = not significant.

Supplementary Table 1. List of predicted *H19*-binding growth-associated microRNAs

A

Growth-inhibitory miRNAs*	Growth-promoting miRNAs*	Bi-functional miRNAs*
let-7a (5,-14.4); let-7b (5,-18.9); let-7c (5,-14.8); let-7d (5,-14.4); let-7f (5,-14.4); let-7g (5,-15.1); let-7i (5,-20.8); miR-100 (3,-22.7); miR-107 (4,-18.0); miR-10a (3,-23.1); miR-125a-3p (4,-12.8); miR-125a-5p (5,-22.5); miR-1271 (7,-18.3); miR-1280 (5,-20.9); miR-1285 (4,-11.3); miR-133a (6,-17.0); miR-133b (6,-17.0); miR-138 (9,-17.0); miR-139-5p (4,-20.0); miR-143 (5,-10.3); miR-145 (4,-24.5); miR-148b (3,-12.7); miR-150 (4,-21.4); miR-152 (3,-13.5); miR-185 (4,-14.5); miR-193b (11,-22.1); miR-194 (1,-12.9); miR-198 (6,-13.2); miR-199a-5p (7,-18.1); miR-199b-5p (7,-14.8); miR-200b (2,-16.3); miR-203 (3,-11.9); miR-204 (7,-21.7); miR-205 (6,-20.4); miR-214 (4,-22.5); miR-218 (9,-17.0); miR-22 (4,-17.6); miR-29b (4,-10.6); miR-320a (7,-18.9); miR-331-3p (11,-24.3); miR-33a (5,-15.2); miR-342-3p (4,-18.4); miR-345 (12,-25.8); miR-34a (5,-23.4); miR-34c-5p (5,-19.5); miR-383 (4,-11.7); miR-409-3p (3,-19.8); miR-449a (5,-23.1); miR-449b (5,-24.5); miR-483-5p (2,-12.6); miR-486-5p (7,-25.9); miR-494 (4,-10.2); miR-498 (10,-24.8); miR-502-5p (10,-23.1); miR-511 (4,-19.3); miR-516a-3p (2,-16.4); miR-519a (3,-12.3); miR-519b-3p (3,-10.4); miR-520b (4,-14.2); miR-520e (4,-14.2); miR-542-3p (4,-12.3); miR-542-5p (5,-21); miR-593 (9,-22.2); miR-596 (7,-24.2); miR-615-5p (7,-28.3); miR-622 (8,-20.8); miR-636 (7,-26.8); miR-637 (20,-29.1); miR-642 (15,-23.4); miR-661 (13,-31.1); miR-874 (13,-31.3); miR-886-3p (6,-17.2); miR-98 (5,-14.4); miR-99a (3,-22.7); miR-99b (3,-27.1)	miR-103 (4,-17.0); miR-1275 (10,-16.0); miR-130b (6,-19.9); miR-135b (3,-13.7); miR-142-3p (4,-13.5); miR-187 (6,-24.1); miR-301a (6,-12.3); miR-328 (10,-33.4); miR-346 (15,-28.4); miR-370 (21,-25.4); miR-373 (4,-21); miR-378 (4,-14.4); miR-423-3p (6,-13.7); miR-454 (6,-14.8); miR-483-3p (17,-27.7); miR-485-3p (3,-13.2); miR-495 (2,-10); miR-520c-3p (4,-15.1); miR-602 (4,-19.7); miR-650 (10,-20.3); miR-657 (5,-23.3); miR-675 (3,-20.2); miR-886-5p (3,-24.9)	miR-125b (5,-18.8); miR-130a (6,-24.2); miR-132 (4,-17.2); miR-135a (3,-13.4); miR-141 (3,-15.3); miR-146a (2,-13.9); miR-146b-5p (2,-16.3); miR-149 (19,-24.9); miR-181b (4,-11.2); miR-184 (9,-12.6); miR-192 (1,-12.6); miR-193a-3p (4,-12.0); miR-197 (6,-24.9); miR-200a (3,-16.9); miR-200c (2,-14.1); miR-210 (1,-21.6); miR-211 (7,-21.7); miR-212 (4,-19.8); miR-215 (1,-11.4); miR-222 (3,-12.6); miR-223 (3,-15.5); miR-24 (10,-15.3); miR-27a (5,-21.0); miR-27b (5,-18.9); miR-296-5p (9,-32.1); miR-330-5p (12,-29.7); miR-372 (3,-18.4); miR-616 (2,-10.4); miR-663 (14,-26.5); miR-708 (4,-12.9); miR-93 (3,-10.7)

B

Growth-inhibitory miRNAs*	Growth-promoting miRNAs*	Bi-functional miRNAs*
let-7a (6,-10.8); let-7b (6,-16.8); let-7c (6,-14.9); let-7e (11,-14.4); let-7g (6,-10.3); let-7i (6,-12.5); miR-107 (6,-10.6); miR-122 (6,-11.2); miR-125a-3p (8,-16.2); miR-125a-5p (5,-19.9); miR-129-5p (2,-11.2); miR-133a (6,-16.8); miR-133b (6,-16.8); miR-139-5p (5,-11.6); miR-145 (8,-20.7); miR-150 (10,-21.6); miR-181d (6,-13.1); miR-185 (13,-13.2); miR-199a-5p (7,-11.1); miR-204 (9,-15.2); miR-205 (16,-14.7); miR-206 (2,-11.5); miR-22 (5,-10.1); miR-331-3p (7,-17.3); miR-345-5p (7,-20.5); miR-34a (9,-13.9); miR-34b-5p (9,-14.7); miR-34c (9,-20.6); miR-362-3p (5,-11.8); miR-375 (2,-11.5); miR-449a (9,-11.1); miR-449b (9,-10.1); miR-486 (5,-12.4); miR-491 (9,-17.9); miR-494 (3,-13.6); miR-503 (3,-12.4); miR-511 (10,-13.7); miR-582-3p (4,-11.3); miR-615-5p (8,-12.1); miR-874 (9,-17.6); miR-92a (5,-11.3); miR-98 (6,-10.7)	miR-103 (6,-10.6); miR-130b (2,-14.4); miR-187 (6,-18.2); miR-328 (7,-12.0); miR-346 (6,-26.3); miR-370 (5,-19.6); miR-423-3p (7,-19.1); miR-485 (8,-13.2); miR-544 (6,-10.1); miR-675-5p (5,-17.3)	miR-125b-5p (5,-15.8); miR-130a (2,-16.9); miR-146a (6,-12.9); miR-149 (13,-19.7); miR-181b (6,-15.5); miR-184 (13,-16.2); miR-197 (8,-26.8); miR-211 (9,-15.2); miR-223 (4,-15.6); miR-296-5p (7,-16.0); miR-330 (5,-12.7); miR-483 (7,-14.7)

List of growth-associated *H19*-binding miRNAs in mammalian species including humans (***A***) and mice (***B***) predicted by *in silico* analysis. *, The data are displayed as "name of the predicted miRNA (number of the predicted binding sites within *H19* sequence, binding score)".

Supplementary Table 2. Pearson Correlation Coefficients (PCC) and their corresponding *P*-values for measuring relationship between the amount of *H19*-bound miRNAs and the level of miRNAs or *H19* expression

Variates (*H19*-absorbed miRNAs)	Covariates (miRNAs or *H19* expression)	PPC	*P* Value
H19-bound Mir34a	Mir34a	0.553	0.255
	H19	0.903*	0.014
H19-bound Let-7e	Let-7e	-0.275	0.598
	H19	0.901*	0.014
H19-bound Let-7g	Let-7g	-0.484	0.330
	H19	0.897*	0.015
H19-bound Let-7i	Let-7i	-0.393	0.440
	H19	0.936**	0.006

*, Correlation between the indicated variate and the indicated covariate is significant at the 0.05 level.
**, Correlation between the indicated variate and the indicated covariate is significant at the 0.01 level.

Supplementary Table 3. List of PCR Primers and oligonucleotide probes

A

Primer Name	Sequence (5'-3')	Application
huGAPDH F1	TGCACCACCAACTGCTTAGC	qRT-PCR
huGAPDH R1	GGCATGGACTGTGGTCATGAG	qRT-PCR
mGAPDH F1	AACTTTGGCATTGTGGAAGG	qRT-PCR
mGAPDH R1	ACACATTGGGGGTAGGAACA	qRT-PCR
h*H19* F1	CGGCCTTCCTGAACACCTTA	qRT-PCR
h*H19* R1	TCATGTTGTGGGTTCTGGGA	qRT-PCR
m*H19* F1	GACTAGGCCAGGTCTCCAGC	qRT-PCR
m*H19* R1	TGACCACACCTGTCATCCTC	qRT-PCR
hu*H19*-CF1	AGCAGGCTCCGAATTCTAGCTGAGGGGCAACCAGGGGAAGATG	Cloning human *H19*
hu*H19*-CR1	AAGCTGGGTCGAATTCATCAGTTATCTAGATGATGAGTCCAGGGCTCC	Cloning human *H19*
m*H19*-ISH-F1	GAGGATGACAGGTGTGGTCA	ISH
m*H19*-ISH-R1	GCTCACCTTGGAGCAGATTC	ISH

B

Probe Name	Sequence (5'-3')	Modification
m*H19*-ASRAP-P1	GGACTTTGCCAGAGCCACTCTTGAACCTTCTTCTAAGTGAATTACGGT GGGTGGGATGTTGTGGCGGCTGGGGACCCATCTGTGTCTTGT	5'-Biotin
m*H19*-ASRAP-P2	CCCGGGGTAGAGGCTTGGCTCCAGGATGATGTGGGTGGTGGTCTCCC GGGTCAGGCAGAGTTGGCCATGAAGATGGATTCTCAGGGGTGG	5'-Biotin

(***A***) Sequences of PCR primers. (***B***) Sequences of oligonucleotide probes for RAP assay